

Magic Numbers of Atoms in Surface-Supported Planar Clusters

Ya-Ping Chiu,^{1,2,*} Li-Wei Huang,¹ Ching-Ming Wei,^{1,2} Chia-Seng Chang,^{1,†} and Tien-Tzou Tsong¹

¹*Institute of Physics, Academia Sinica, Taiwan, Republic of China*

²*Institute of Atomic and Molecular Sciences, Academia Sinica, Taiwan, Republic of China*

(Received 2 March 2006; published 18 October 2006)

Surface-supported planar clusters can sprout active research and create numerous applications in the realm of nanotechnology. Exploitation of these clusters will be more extended if their properties on a supported substrate are thoroughly apprehended, and if they can be fabricated in a controllable way. Here we report finding the magic numbers in two-dimensional Ag clusters grown on Pb quantum islands. We demonstrate, with the images and energy spectra of atomic precision, the transition from electronic origin to a geometric one within the same system. Applying the magic nature, we can also produce a large array of planar clusters with well-defined sizes and shapes.

DOI: [10.1103/PhysRevLett.97.165504](https://doi.org/10.1103/PhysRevLett.97.165504)

PACS numbers: 61.46.Bc, 07.79.Cz, 73.22.-f, 81.16.Dn

Magic numbers in gas phase clusters of alkali atoms were predicted theoretically [1] and experimentally observed in mass spectrometry [2] in the 1980s. Many intriguing properties associated with these clusters in terms of ionization potential, chemical reactivity, and photoabsorption effectiveness have, since then, been investigated extensively [3–9]. It has been shown that the catalytic property of these clusters can change drastically with addition or subtraction of a single atom. Electronic shell-closing effects are successfully used to explain the sequence of the magic numbers when metal clusters are small and the electronic energy dominates [10]. For larger clusters, the packing related to the atomic arrangement becomes more important which gives rise to the geometrical shell structure [11–13]. The threshold of this transition for gas phase clusters usually occurs as the cluster size exceeds a few thousands of atoms. Magic numbers have also been found in mass production of photo-fragmented bimetallic clusters [14]. A specific number of six was found and a planar triangular configuration was proposed for these clusters. However, although many theoretical studies have predicted the existence of two-dimensional (2D) clusters with magic numbers of atoms on supported substrates [15,16], formation of such clusters has never been realized.

Meanwhile, in quest of fabricating ever smaller devices, the mass production of surface-supported minute elements with uniform size, shape, and chemical homogeneity becomes enormously important and challenging [17]. As the size of the element approaches nanometer scale, the uncertainty of even an atom in number or position can alter its property significantly. It is thus highly desirable that in nanoscience research both the fabrication process and property measurements achieve the atomic precision. Self-organized growth is an attractive approach where a large number of similar nanostructures can be made simultaneously. A routine practice is to identify some key factors from numerous kinetic processes involved in the growth. Judicious tuning of these factors is then used to steer the growth. In order to achieve a uniform spatial arrangement,

suitable templates are normally employed. Regular strain-relief dislocations [18] and periodic surface reconstructions [19,20] have all been applied in an attempt to improve the quality of self-organized growth. Except for the self-assembly of supramolecular nanostructures of noncovalent bonding [21], the self-organized growth with a template and adjustable growth parameters alone still proves difficult in defining the size and shape of the nanostructures to atomic precision.

Recently, we have found that periodic electronic patterns formed on Pb quantum islands can serve as the templates for spontaneous growth of metallic nanoclusters [22]. The Pb islands are grown at low temperature on the Si (111) surface passivated with an incommensurate Pb atomic layer. Because of the lattice mismatch between Pb and Si, a superstructure with a periodicity of 3.84 nm is formed. Black lines in the Fig. 1(a), running across the brightest points of the superstructure, outline a unit cell. The rhombic unit cell can be further divided into two triangular halves as shown by the white dashed lines. At the interface one has the face-centered cubic (fcc) stacking while the other the hexagonal close-packed (hcp) stacking. With regard to diffusion for Ag atoms on this surface of the Pb islands, a steep binding potential difference exists between these two halves. Owing to this difference, the confined nucleation has taken place at the fcc halves exclusively [23]. Thus, highly ordered arrays of single-atomic-layer thick Ag nanoislands (nanopucks) can be produced spontaneously on these Pb islands. Although the sites of the nanopucks are precisely defined by the template, the size and shape of these Ag nanopucks display a clear disparity under atomic resolution.

Since the averaged size of these Ag nanopucks is around 2 nm, which is comparable to the electronic Fermi wavelength, the lateral confinement of Ag nanopucks should have an essential influence on their electronic structures. We thus perform tunneling spectroscopy on individual nanopucks of various sizes. The correlation between the shape and size of an Ag nanopuck and its electronic structure is thoroughly investigated and, along the study,

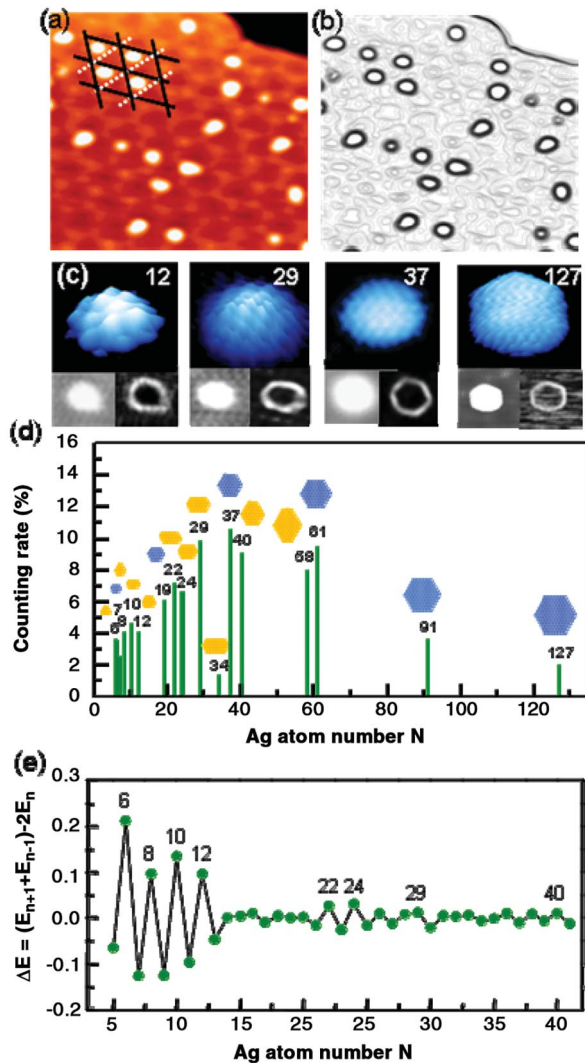


FIG. 1 (color). (a) Ag nanopucks possessing various shapes and sizes grown on Pb quantum islands. The black lines outline the unit cell of the superstructure and each unit cell is divided into two triangular halves by the white lines. (b) The corresponding shapes of Ag nanopucks in (a). The shapes are highlighted by differentiation. (c) AtOMICALLY resolved images of Ag magic nanopucks with 12, 29, 37, and 127 atoms. The corresponding STM images and shapes are shown in the insets. (d) The size distributions of over a thousand Ag nanopucks grown on Pb quantum islands. The schematic structures are drawn above each magic number for the most frequently observed ones. The sketches are divided into two based on the attributed factors: geometrical effect (painted in blue) and electronic effect (painted in orange). (e) The calculated stability function for the ground state Ag nanopucks up to atom numbers of 41.

we discover the magic numbers in 2D surface-supported nanoclusters. Here we will reveal unambiguously the origin of these magic numbers and the trend of transition from the electronic closed shell effect to the ideal geometrical arrangement. We will also demonstrate that the method of self-organized growth can achieve atomic precision by utilizing the magic nature associated with the growth of

Ag nanopucks on the suitable template of Pb quantum islands.

The experiments are performed with a variable-temperature scanning tunneling microscopy (STM) under an ultrahigh vacuum with the base pressure 5×10^{-11} torr. The system is also equipped with Pb and Ag e -beam evaporators. The stripe incommensurate phase (SIC) is prepared by depositing slightly more than one monolayer (ML) of Pb on a clean Si(111)-(7 \times 7) surface at room temperature followed by annealing the sample to 700 K. The sample is then cooled to about 200 K and an extra amount of Pb is further added to produce Pb quantum islands. On top of these islands, Ag nanopucks are fabricated with predetermined growth parameters. STM is used to obtain atOMICALLY resolved images. The local electronic density of states of an Ag nanopuck is measured at 100 K by taking the first derivative of the tunneling current (dI/dV) as a function of the sample bias.

We also carry out first-principles total energy calculations for isolated Ag nanopucks of various sizes and shapes, based on the density functional theory (DFT) with the proposed generalized gradient approximation (GGA) by Perdew, Burke, and Ernzerhof [24]. The single-particle Kohn-Sham equations [25] are solved using the plane-wave-based Vienna *ab initio* simulation program (VASP) [26]. The interactions between the ions and valence electrons are described by the projector augmented-wave (PAW) method in the implementation of Kresse and Joubert [27]. The energy cutoff for the plane-wave basis is 250 eV. All Ag clusters were simulated by being placed in the center of rectangular supercells which are large enough to neglect cluster-cluster interactions, i.e., a spacing of at least 10 Å separated by vacuum between the atoms of neighboring clusters. As the supercells are large enough, only one k at the gamma point is included in the Brillouin-zone integration. Relaxation processes in optimizing static structures are accomplished by requiring all atomic forces are smaller than 0.02 eV/Å and the total energy is converged to 1×10^{-5} eV.

Figure 1(a) displays the STM image of a few Ag nanopucks on Pb quantum islands with Ag deposition flux of 0.1 ML per minute at 100 K and slowly annealed to 170 K. Their shapes are made prominent by differentiating the topographic image to highlight the boundaries [Fig. 1(b)], and their atOMICALLY resolved images are shown in Fig. 1(c). Even with these images of high resolution, the counting of the atom number could be uncertain, especially near the edge of a cluster. However, careful examination finds existence of some special sizes and shapes, and the size of these clusters is tied with a specific shape. The atomic number of a cluster is hence determined by both the vigilant atom-counting and its outlook. We have employed the same growth recipe to produce over a thousand Ag nanopucks and their size distribution is plotted in Fig. 1(d). The most dramatic discovery is the existence of magic numbers in this histogram. The corresponding size and

shape of a nanopuck are drawn with the distribution peaks. As is apparent, the closely packed hexagons (painted in blue) spread over the whole range with the numbers of 7, 19, 37, 61, 91, and 127. These numbers follow the formula $N = 1 + 6\sum s$, where s is the shell number, and are representative of the 2D geometrical shell-closing structures. Below the atom number of 60, other magic numbers 6, 8, 10, 12, 22, 24, 29, 34, 40, and 58 (painted in orange) are found. Our calculations indicate the clusters with numbers less than 60 are resulted from the close-shell electronic structures with large energy gap (>0.17 eV) near the Fermi level. When the nanopucks are small, the electronic energy closely associated with the size and shape is the major attribute to its total energy, but this factor gives way to the geometric shell-closing structure at the larger atom numbers. The transition number begins at around 60 atoms, which is much smaller than that for the free spherical clusters. This is because the three-dimensional cluster has much higher degeneracy and subsequently much larger gaps between the shells [15].

In order to explore the origin of these magic numbers, two magic sizes of nanopucks are selected for detailed study. Spatially averaged tunneling spectra for the nanopucks containing 24 Ag atoms and 29 atoms [referring to Fig. 2(a)] are measured near the centers of these nanopucks, respectively. If the peaks in the spectra are extracted (marked with black bars) and compared with the calculated ones (red bars), the agreements are grossly good considering the calculations have not taken the substrate effect into account. These results indicate the 2D nature of the Ag nanopucks has been largely preserved. However, the electronic Moirè pattern on the substrate has differentiated one half of a unit cell from the other in binding strength to the Ag adatoms. It seems that this binding trap has only a mean-field effect on the Ag nanopuck, especially when the puck is small. We therefore calculate the electronic energy for each nanopuck up to 41 atoms. A stability function is defined using the second difference in total energy as $\Delta E(N) = E(N+1) + E(N-1) - 2E(N)$, where N is the number of atoms in the nanopuck. Once this function is plotted against N , several peaks are observed as shown in Fig. 1(e). Thus the experimental magic numbers agree almost perfectly with the theoretical calculations. This fact reinforces our confidence in determining the atom number of a nanopuck.

A further analysis shows the calculated electronic states near the Fermi level originate mainly from the confinement of Ag $5s$ electrons. These states can change with the atomic arrangement of a nanopuck. Those drawn shapes in Fig. 1(d) are the most frequently ($>95\%$) found structures at each magic numbers by the experiment and closely correspond to one of the calculated ground state structures. As the cluster size grows larger, its shape tends to conform to the symmetry of the substrate potential, considering that the boundary of the fcc triangular half cell excluding the three apexes of higher potential delineates a hexagonal shape. In addition, crowding of the discrete states near

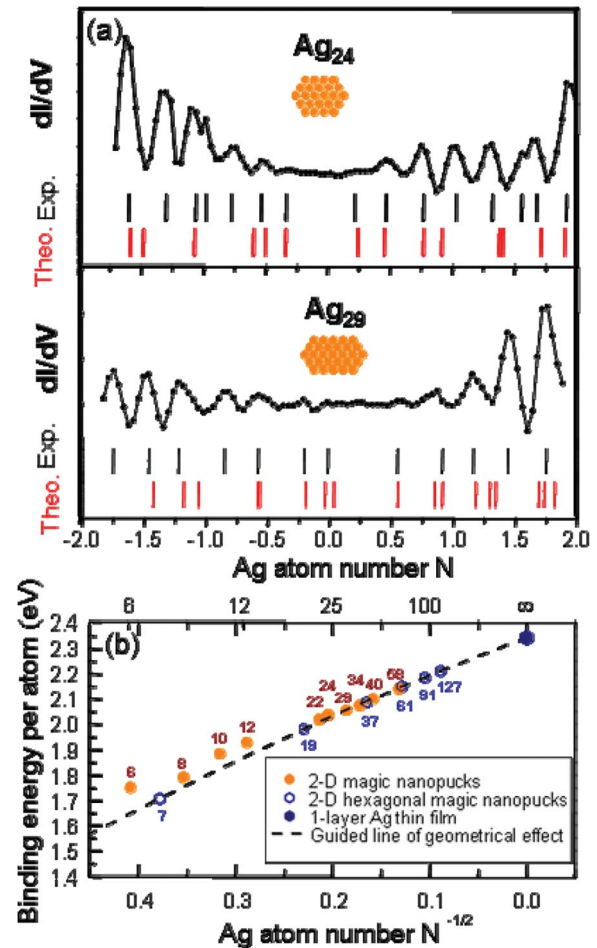


FIG. 2 (color). (a) Spatially averaged tunneling spectra for Ag nanopucks with 24 and 29 atoms. Peaks in the spectra are plotted with black bars. The corresponding local density of states calculated for two-dimensional Ag disks with the experimentally observed shapes in red bars. (b) Binding energy per atom as function of Ag cluster size. The dotted line is a fit through ideal geometrical structures, separating the stable clusters from the unstable, and only those stable ones are displayed.

the Fermi level will lessen the weighting of electronic contribution, and assuming of the crystalline bonding nature will augment the effect of geometric arrangement. All these factors favor the transition from the close-shell electronic structures to ideal geometric ones. We have calculated the binding energy per atom as function of the nanopuck size as plotted in Fig. 2(b). The binding energy increases monotonically with the size in general and the dotted line is a fit through the hexagonal structures. This line separates the stable clusters from the unstable and only those stable ones are displayed in the figure. Our calculations show that, for smaller clusters, the electronic shell-closing effect plays a decisive role in determining the stability of a cluster. When this effect fades out as the cluster size becomes larger than 60 atoms, the only stable structures left are of hexagonal shapes, which are called ideal geometric structures. We thus attribute the formation

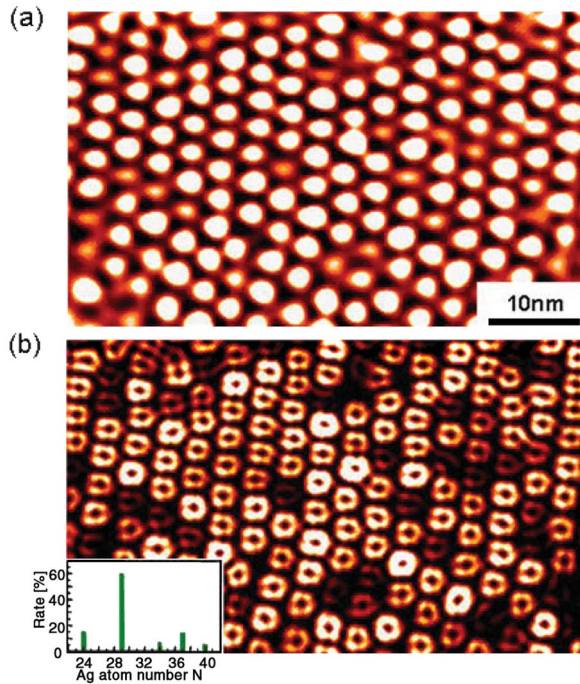


FIG. 3 (color). (a) A large array of two-dimensional Ag nanopucks fabricated with magic numbers of 24, 29, 34, 37, and 40 atoms. (b) Differentiating the corresponding topography image, the uniformity in size and shape of the nanopucks is emphasized. Inset: histogram for size distribution.

of ideal structures to the effect of geometric shell closing in analogy to the electronic shell closing.

In self-organized growth, kinetic processes are the key to control the size and shape of the grown clusters. The existence of magic numbers in the cluster creates a leeway in which a better overall control can be exercised. We thus attempt to prepare as uniformly and widely distributed Ag nanopucks as possible by judiciously tuning the growth parameters, i.e., with a flux of 0.1 ML/min, total dosage of 0.2 ML, growth temperature of 100 K, and followed with annealing to 170 K. Figure 3 shows what has been achieved. In this 60 nm \times 35 nm image, over 150 nanopucks are fabricated. They are found to disperse within five magic numbers. According to the distribution histogram (see the inset), 60% of the nanopucks are of 29 atoms, 15% 24 atoms, 15% 37 atoms, 6% 34 atoms, and 4% 40 atoms. The differential image [Fig. 3(b)] indicates that the shapes of these nanopucks are quite uniform as well.

In conclusion, magic numbers in surface-supported two-dimensional Ag nanoclusters have been discovered. Detailed calculations based on first-principles density functional theory have been made to illuminate the origin of the magic number. They originate from the electronic shell-closing effect when the cluster is small. As the Ag nanopuck grows to a certain size, the geometrical effect takes hold from the electronic effect as the major attribute. By combining the magical nature of size-dependent Ag nanopucks with the suitable Pb island substrate, planar clusters

in restricted magic numbers and shapes can be produced in an ordered array.

The authors would like to thank M. Y. Chou for insightful discussion. This work was supported by the NSTP for Nanoscience and Nanotechnology through the National Science Council and by the Program for Promoting University Academic Excellence through Ministry of Education, Taiwan, Republic of China.

*Current address: Department of Physics, National Sun Yat-Sen University, Kaohsiung, Taiwan, Republic of China.

†Email address: jasonc@sinica.edu.tw

- [1] W. Ekardt, Phys. Rev. Lett. **52**, 1925 (1984).
- [2] W. D. Knight *et al.*, Phys. Rev. Lett. **52**, 2141 (1984).
- [3] P. Jena, B. K. Rao, and S. N. Khanna, *Physics and Chemistry of Small Clusters* (Plenum, New York, 1987).
- [4] Xi. Li, H. Wu, X. B. Wang, and L. S. Wang, Phys. Rev. Lett. **81**, 1909 (1998).
- [5] M. Haruta, Catal Today **36**, 153 (1997).
- [6] C. Yannouleas and U. Landman, Phys. Rev. Lett. **78**, 1424 (1997).
- [7] C. T. Campbell, S. C. Parker, and D. E. Starr, Science **298**, 811 (2002).
- [8] N. Niliius, T. M. Wallis, and W. Ho, Science **297**, 1853 (2002).
- [9] K. E. Schriver, J. L. Persson, E. C. Honea, and R. L. Whetten, Phys. Rev. Lett. **64**, 2539 (1990).
- [10] W. A. de Heer, Rev. Mod. Phys. **65**, 611 (1993).
- [11] T. P. Martin, T. Bergmann, H. Goehlich, and T. Lange, J. Phys. Chem. **95**, 6421 (1991).
- [12] P. Stampfli and K. H. Bennemann, Phys. Rev. Lett. **69**, 3471 (1992).
- [13] A. L. Mackay, Acta Crystallogr. **15**, 916 (1962).
- [14] E. Janssens, H. Tanaka, S. Neukermans, R. E. Silverans, and P. Lievens, New J. Phys. **5**, 46 (2003).
- [15] C. Kohl, B. Montag, and P.-G. Reinhard, Z. Phys. D **38**, 81 (1996).
- [16] S. M. Reimann, M. Koskinen, H. Häkkinen, P. E. Lindelof, and M. Manninen, Phys. Rev. B **56**, 12 147 (1997).
- [17] J. V. Barth, G. Costantini, and K. Kern, Nature (London) **437**, 671 (2005).
- [18] H. Brune, M. Giovannini, K. Bromann, and K. Kern, Nature (London) **394**, 451 (1998).
- [19] M. Y. Lai and Y. L. Wang, Phys. Rev. Lett. **81**, 164 (1998).
- [20] J. L. Li *et al.*, Phys. Rev. Lett. **88**, 066101 (2002).
- [21] T. Yokoyama, S. Yokoyama, T. Kamikado, Y. Okuno, and S. Mashiko, Nature (London) **413**, 619 (2001).
- [22] H. Y. Lin *et al.*, Phys. Rev. Lett. **94**, 136101 (2005).
- [23] Y. P. Chiu, H. Y. Lin, T. Y. Fu, C. S. Chang, and T. T. Tsong, J. Vac. Sci. Technol. A **23**, 1067 (2005).
- [24] J. P. Perdew, K. Burke, and M. Ernzerhof, Phys. Rev. Lett. **77**, 3865 (1996).
- [25] W. Kohn and L. J. Sham, Phys. Rev. **140**, A1133 (1965).
- [26] G. Kresse and J. Hafner, Phys. Rev. B **47**, 558 (1993); **49**, 14 251 (1994); G. Kresse and J. Furthmuller, *ibid.* **54**, 11 169 (1996); Comput. Mater. Sci. **6**, 15 (1996).
- [27] G. Kresse and D. Joubert, Phys. Rev. B **59**, 1758 (1999).